Water and the *Huisgen* Cycloaddition Reaction: A Focus on Polar Contributions to the Transition State in the Reactions of Dicyano(phthalazinium)methanide with Substituted Styrenes and Benzylidene Acetones

by **Richard N. Butler***[a]), **Anthony G. Coyne**[a]), **William J. Cunningham**[a]), **Eamon M. Moloney**[a]), and **Luke A. Burke**[b])

[a]) Chemistry Department, National University of Ireland, Galway, Ireland
[b]) Chemistry Department, Rutgers University, Camden, New Jersey 08102, USA

Dedicated to *Rolf* and *Trudl Huisgen*

Synthetic and kinetic studies on the 1,3-dipolar cycloaddition reactions of dicyano(phthalazin-2-ium-2-yl)methanide (**1**) with some substituted styrenes and 'benzylidene acetones' in MeCN and H_2O containing 10 mol-% of MeCN are reported. The kinetic data were supported by theoretical calculations. The major products from styrenes were *exo*-2-aryl-1,2,3,10b-tetrahydropyrrolo[2,1-*a*]phthalazine-3,3-dicarbonitriles **3**, and, from 'benzylidene acetones', 1-*endo*,2-*exo*-2-acetyl-1-aryl-1,2,3,10b-tetrahydropyrrolo[2,1-*a*]phthalazine-3,3-dicarbonitriles **7**. There was no indication that the cycloadditon transition states were more polar in the aqueous environment than in MeCN.

Introduction. – The *Huisgen* [3 + 2] cycloaddition reaction [1] permeates the whole chemistry, from permanganate based synthesis of 1,2-diols, to ozone based synthesis of carboxylic acids, to synthesis of extensive ranges of mono and fused five-membered-ring systems. The ubiquitous normal [3 + 2] cycloaddition reactions ($HOMO_{dipole}$ control) pass through concerted asynchronous transition states and are relatively insensitive to solvent polarity. The solvent-polarity influences on their rates are often two to three orders of magnitude smaller than for cycloadditions that pass through dipolar or diradical intermediates, as assessed (for dipolar aprotic solvents) by means of the *Dimroth – Reichardt* E_T solvent-polarity parameters [2].

While studying synthetic cycloaddition – rearrangement sequences with azolium- and azinium ylide 1,3-dipoles, where two of the 1,3-dipole π-electrons are embedded in an azole or azine ring, we found that the yellow-coloured, highly stable molecules of type **1** (= dicyano(phthalazin-2-ium-2-yl)methanide) and **1A** were particularly favourable substrates for extensive UV/VIS kinetic studies in the reactions leading to adducts **2** and **3** (*Scheme 1*) [3]. For the 1,3-dipole **1**, a plot of log k_2 against the ionisation potential (representing the HOMO energy) for 26 dipolarophiles gave a classic *Sustmann* type-II U-shaped curve. The 1,3-dipole **1** can react in either $HOMO_{dipole}$ or $LUMO_{dipole}$ mode with electron-poor and electron-rich dipolarophiles, respectively (*Scheme 1*) [3].

We decided to examine the influence of adding H_2O to the organic solvent for these reactions. For the dipole **1**, the effect of H_2O could be followed up to a mol fraction of 0.9 [4], but to peform the reactions in neat H_2O, the fused benzene ring in **1** had to be

Scheme 1

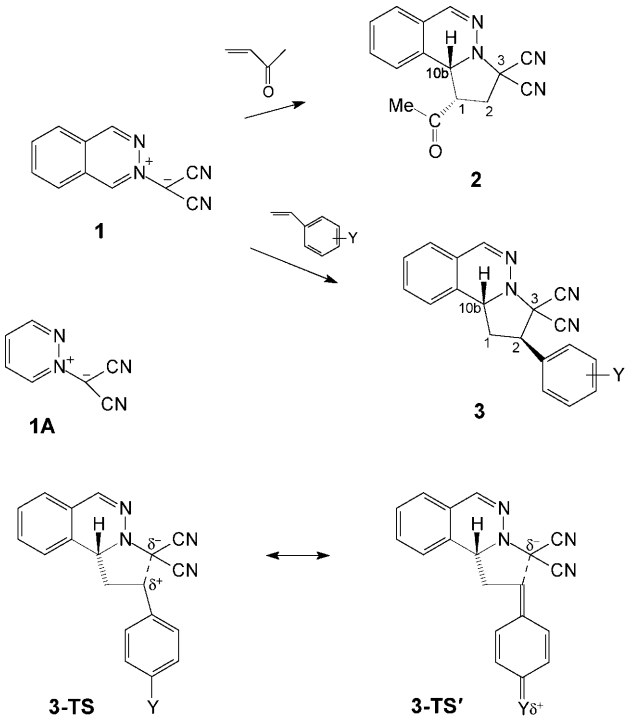

removed [5]. The resulting substrate **1A** is a *Sustmann* type-I 1,3-dipole, reacting *via* the $HOMO_{dipole}$ mode with electron-poor dipolarophiles only. This change did not influence the water effect on the cycloaddition reactions, which were quite comparable for both substrates **1** and **1A**. Experimental comparisons of rates for the reactions of **1** and isoquinolinium dicyanomethanide with but-3-yn-2-one, ethyl vinyl ketone (EVK), methyl acrylate (MA), and *N*-methylmaleimide as representative examples, as well as theoretical calculations, showed that the second, nonquaternised N-atom in **1** and **1A** does not play a role in the observed water effects. When the rates of reaction for the dipoles **1** and **1A** with a wide range of dipolarophiles were compared in H_2O and MeCN or acetone, the dipolarophiles were grouped into 'water-super' and 'water-normal' types, based on the magnitude of their response to H_2O [4]. The rate increases in H_2O for the former were about ten times higher than for the latter. For example, at 37°, k_{H_2O}/k_{MeCN} for the reaction of the dipole **1A** with EVK ('water-super') was 164, as compared to 15.3 for the reaction with MA ('water-normal') [5]. We chose this terminology for dipolarophiles to distinguish the magnitude of their H_2O response, reflecting the term 'superdipolarophile' coined by *Huisgen* and co-workers [6] to describe the extraordinary reactivity of thiones as dipolarophiles in [3+2] cycloadditions. This type of H_2O response is also seen in *Diels–Alder* reactions. *Breslow* and *Rideout* reported rate responses to H_2O for the cycloaddition reactions of methyl vinyl ketone (MVK) with cyclopentadiene, $k_{H_2O}/k_{isooctane}$ being 722 at 20°; and the

comparable rate ratio for the cycloaddition of cyclopentadiene with acrylonitrile was 31 (at 30°) [7].

The exponential nature of the late rate enhancements caused by gradually increasing the mol fraction of H_2O in the solvent from 0 to 1 for the separate cycloaddition reactions of the 1,3-dipole **1A** with EVK and MA in the solvents MeCN, acetone, MeOH, EtOH, and *t*-BuOH, as well as temperature effects and theoretical calculations, led us to conclude that the essential difference between 'water-super' and 'water-normal' dipolarophilic behaviour is due to a H-bonding growth of strong H_2O clusters around the 'water-super' dipolarophile in the transition state (TS). With 'water-normal' dipolarophiles, H_2O clusters can also grow, but they are weak, and as more bridging H_2O molecules are added, the weak clusters drift away from the H-bond-acceptor sites on the dipolarophile [5]. H-Bonding-promoted water-cluster growth is a special effect in the reactions of **1** and **1A**, which is added to the all-pervasive and ubiquitous hydrophobic effect that dominates organic reactions in aqueous media [8–10]. *Breslow* and co-workers have developed a deep understanding of the hydrophobic effect on organic reactions [7][8], and established a method of diagnosing its presence using special salt-effects [9]. These salt-effect tests, when applied to the reactions of the 1,3-dipole **1A** in H_2O, support the presence of hydrophobic contributions [4]. Increasing understanding of the hydrophobic effect has now progressed, so that it can be used as a probe of reaction mechanisms and regioselectivity [10][11].

In the case of the *Huisgen* cycloaddition, H-bonding effects may also oppose the hydrophobic effect, as occurs with benzonitrile oxides, where the 1,3-dipole has strong H-bond acceptor sites, and small H_2O rate-enhancements or -inhibitions are observed, with no dramatic differences between dipolarophile types [12]. Beside hydrophobic [8] and special H-bonding effects [5][13–15], which may contribute to the effects of H_2O on organic reactions, the question also arises whether there is an increase in the polarity of the transition state, when organic reactions are carried out in H_2O. Since growth of H_2O clusters plays a major role in the reactions of 'water-super' dipolarophiles with **1**, we wished to consider whether there might be a cooperative increase in the polarity of the transition state, as each bridging H_2O molecule is fastened strongly into the growing solvent cluster around the transition state. For the reaction of cyclopentadiene with 1,4-naphthoquinones, *Engberts* and co-workers [16] concluded that charge separation in the activated complex is not much different from that in organic solvents, but for *Diels–Alder* reactions of a di(pyrid-2-yl)-1,2,4,5-tetrazine (a substrate with six H-bond-acceptor sites), the transition-state polarity may be increased in aqueous media [17].

Results and Discussion. – 1. *Substituted Styrenes.* In principle, it should be easy to determine, *via Hammett* ρ values, whether transition states are more polar in H_2O than in organic solvents. In practise, however, this is usually far from easy. For the reactions of the 1,3-dipole **1** with *para*-substituted *N*-phenylmaleimides, we found that the rate correlated well with σ^0 values, providing a ρ value in MeCN of $+0.15$, and a ρ value of $+0.08$ in H_2O/MeCN 9:1[1]), indicating little charge in the transition state, and no change in the aqueous medium [4].

---

[1]) All solvent ratios refer to a molar basis.

In order to move the substituents closer to the reaction centre, we have attempted similar measurements with substituted styrenes. The kinetics results are shown in *Table 1* and *Fig. 1*. Experimental difficulties, particularly connected with insolubility, severely limited the rate measurements in H_2O/MeCN 9:1. Styrene is at the bottom electron-rich side of the *Sustmann* U-shaped curve [3], and the *Hammett* plot reflects the mechanistic changeover between the $HOMO_{dipole}$ and $LUMO_{dipole}$ modes, the right and left sides of *Fig. 1* respectively.

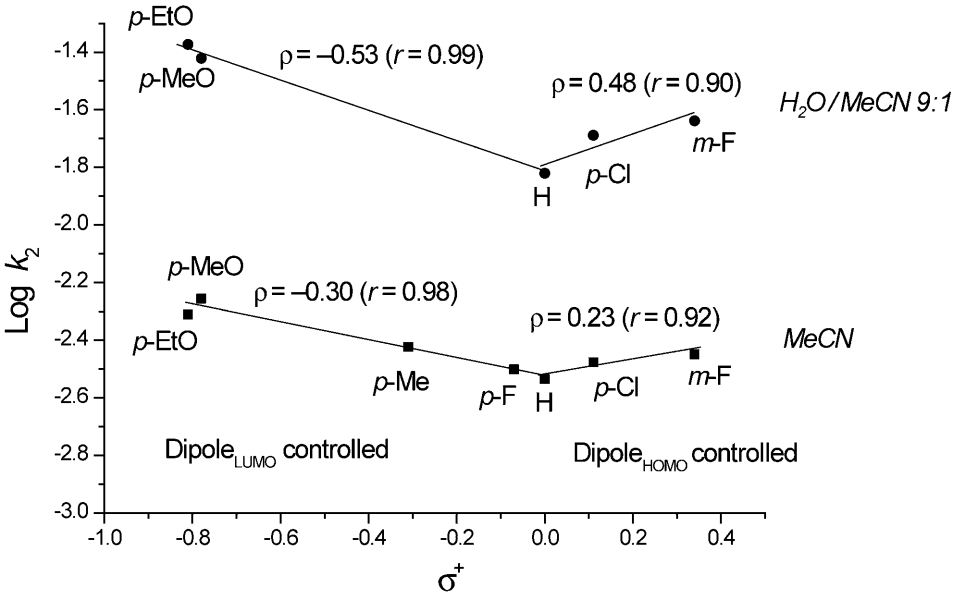

Fig. 1. *Experimental* Hammett *data for the reaction of* **1** *with substituted styrenes* (see *Scheme 1*)

Table 1. *Kinetic and Synthetic Data for the Reaction of* **1** *with Styrenes of Type* $Y-C_6H_4-CH=CH_2$ (see *Scheme 1*)

Entry	Y	Compd.	$k_2 \times 10^{-3}$ [l mol^{-1} s^{-1}][a])		Total yield [%][b])	
			MeCN	H_2O/MeCN 9:1	MeCN	H_2O
1	H	**3a**	2.92	15.1	87 (5.7)[c])	78 (6.1)
2	*p*-MeO	**3b**	5.55	37.8	71 (7.8)	87 (8.6)
3	*p*-EtO	**3c**	4.98	42.3	–	–
4	*p*-Me	**3d**	3.77	–	–	–
5	*m*-F	**3e**	3.56	22.9	91 (5.1)	82 (6.4)
6	*p*-Cl	**3f**	3.34	20.4	–	–
7	*p*-F	**3g**	3.15	–	–	–
8	*m*-NO_2	**3h**	–	–	79[d]) (6.2)	–

[a]) Determined at 37°. [b]) Sum of *endo*- and *exo*-isomers; at 80°. [c]) In parentheses, ratio *exo*/*endo*. [d]) The other regioisomer was also formed in 6% yield (see *Exper. Part*).

When faced with experimental limitations, theoretical calculations provide assistance. Theoretical calculations were carried out with the Gaussian03 series of

programs (B3LYP/6-31G(d) method) [5]. A computer output for each calculation can be downloaded from http://camchem.rutgers.edu/~burke. Care was taken that the aryl substituents were internally oriented the same way in the reactants and the transition-state (TS) structures. Only *para*-substituents were considered for the *Hammett* study. Although the '2-*exo*' isomer was clearly preferred energetically, the other three isomers were studied for Y = *p*-NH_2, *p*-Cl, and *p*-NO_2 (see *Scheme 1*). The *meta*-NO_2 case was also studied to compare rates of the four possible isomers with experiment (*Table 1*). The *meta*-NO_2 group was maintained in the '*cis*' position relative to the vinyl group.

Table 2 reports the activation energies E_a, activation entropies S_a, and activation free energies G_a. Also included in *Table 2* are the *Hammett* σ values, and enhanced σ^+ and σ^- values employed. Two types of rate ratios are reported. When comparing isomer ratios in rate-controlled processes using transition-state-theory, free-energy values should be used (assuming the pre-exponential factors are equal):

$$k_1/k_2 = e^{(G_{a1}/RT)}/e^{(G_{a2}/RT)} \quad (1)$$

In contrast, when constructing *Hammett* plots, E_a should be used (assuming the *Arrhenius* pre-exponential factors are equal):

$$k_1/k_2 = e^{(E_{a1}/RT)}/e^{(E_{a2}/RT)} \quad (2)$$

The calculated relative rates for isomers in styrenes show a general 10:1 ratio for *exo*/*endo* formation in 2-position, comparable to experiment (*Table 1*). In the *p*- and *m*-NO_2 cases, competition for the opposite isomer appears, in agreement with the experimental results for *meta*-nitrostyrene, but not for the relative *exo*/*endo* ratio in the 1-regioisomer. It is possible that a dipolar solvophobic effect is predominant in the minor 1-regioisomeric case (which is *endo*), where solvent accessibility is more important to the *exo*/*endo* ratio. In contrast, in the major 2-regioisomer, the aryl group protrudes in both the *exo*- and *endo*-stereoisomers, and has comparable solvent accessibility in each case (see *Sect. 2* below).

Plots of E_a *vs.* σ^+ show a better correlation ($R^2 = 0.978$) than with ordinary σ values (U-shaped, $R^2 = 0.689$) for electron-donating (ED) groups by resonance (including *p*-Cl and *p*-F), as shown in *Fig. 2,a*. Plotting electron-withdrawing (EWD) groups (by resonance) with σ^0 or σ^- *Hammett* values shows a distinctly flat grouping, with little correlation ($R^2 = 0.049$). Unsubstituted styrene was included in both correlations. *Fig. 2,b* gives a plot of the same *Hammett* values, but against the logarithm of the ratio of rate constants of substituted to unsubstituted styrenes. Also included are those ratios for the substituents that were used both in the experiment (*Table 1*) and theory (*Table 2*). The slopes of the lines give the *Hammett* ρ^+ values, which are -0.86 (theoretical) and -0.29 (experimental). The reaction is not sensitive to substitution by EWD groups (by resonance).

Fig. 3 shows plots of the four unsubstituted styrene TS structures, and gives the distance (in Å) for the two new bonds being formed. The *exo*- and *endo*-forms of the preferred 2-stereoisomer give distinctly different bond lengths, whereas they are nearly equal in the two 1-stereoisomers. In the preferred cases, the styrene CH_2 group's new bond is *ca.* 0.7 Å shorter than the other, leaving a certain amount of resonance

Table 2. *Theoretical Calculations for Substituted Styrenes of Type* $Y-C_6H_4-CH=CH_2$ (see *Scheme 1*). Activation energy E_a in kJ mol^{-1}, activation entropy S_a in J mol^{-1} K^{-1}, free energy of activation G_a in kJ mol^{-1}.

Y	Aryl position	E_a	$-S_a$	G_a	Z[a])	σ^0	σ^+ or σ^-	k_Y/k_H[b])	$\log(k_Y/k_H)$	
									calc.	exper.
H	1-*exo*	61.69	206.26	126.39	0.02					
	2-*exo*	55.10	193.15	115.81	1.00	0.00	0.00	1.00	0.00	0.00
	1-*endo*	70.90	201.61	133.71	0.00					
	2-*endo*	60.11	195.23	121.53	0.11					
p-NMe_2	2-*exo*	45.69	183.19	104.26		−0.32	−1.70	38.53	1.59	
p-NH_2	1-*exo*	63.07	202.15	126.40	0.00					
	2-*exo*	49.38	183.28	106.86	1.00	−0.30	−1.30	9.23	0.96	
	1-*endo*	72.15	198.99	134.27	0.00					
	2-*endo*	52.38	190.46	112.44	0.11					
p-OH	2-*exo*	51.39	222.25	110.38		−0.22	−0.92	4.63	0.67	
p-Me	2-*exo*	51.33	184.46	109.51		−0.14	−0.30	1.77	0.25	0.11
p-MeO	2-*exo*	53.62	202.47	117.06		−0.12	−0.78	4.33	0.64	0.28
p-F	2-*exo*	54.64	191.82	115.00		0.15	−0.07	1.20	0.08	0.03
p-Cl	1-*exo*	62.36	203.55	125.94	0.02					
	2-*exo*	55.83	190.56	115.74	1.00	0.34	0.11	0.75	−0.12	0.06
	1-*endo*	70.72	199.61	132.99	0.00					
	2-*endo*	60.56	195.14	121.94	0.09					
p-CHO	2-*exo*	55.96	196.65	117.63		0.47	1.04	0.72	−0.14	
p-Ac	2-*exo*	56.07	191.45	116.18		0.47	0.82	0.69	−0.16	
p-CF_3	2-*exo*	56.69	194.50	117.74		0.53	0.65	0.54	−0.27	
p-CN	2-*exo*	56.23	193.63	117.06		0.65	1.46	0.93	−0.03	
p-NO	2-*exo*	55.28	195.93	116.81		0.71	0.99	0.65	−0.19	
p-NO_2	1-*exo*	59.43	203.43	122.93	0.09					
	2-*exo*	56.38	192.25	116.72	1.00	0.81	1.23	0.61	−0.22	
	1-*endo*	65.98	198.51	127.75	0.01					
	2-*endo*	60.18	196.96	122.03	0.13					
m-NO_2	1-*exo*	60.30	203.79	124.22	0.03					
	2-*exo*	54.11	194.79	115.33	1.00					
	1-*endo*	71.92	198.03	135.31	0.00					
	2-*endo*	57.17	198.42	119.58	0.19					

[a]) Ratio $k_{isomer}/k_{2\text{-exo}}$, *i.e.*, ratio of the rate constant for the formation of any isomeric product to that for the formation of the 2-*exo* product (*Eqn. 1*). [b]) According to *Eqn. 2*.

stabilisation of the CH group by the aryl ring. There is very little variation of this ratio in the substituted styrenes. Given that resonance forms of the dipole place a negative charge on the two atoms involved in bond formation, it is not surprising that ED groups, which stabilize a positive charge on the styrene CH group by resonance, should lower the activation energy of the reaction, and give a correlation with enhanced σ^+ *Hammett* values (see *Scheme 1*, resonance forms 3-TS and 3-TS′).

When various Polarisable-Continuum methods were tested to assess the influence of increased polarity of the medium (mimicking the possible influence of a H_2O environment), the TS structures became too flexible for the optimisation procedures, and the calculations did not lead to a conclusion. The available experimental results in H_2O/MeCN 9:1 (*Fig. 1*) suggest that the transition state is not significantly more polar in aqueous environment.

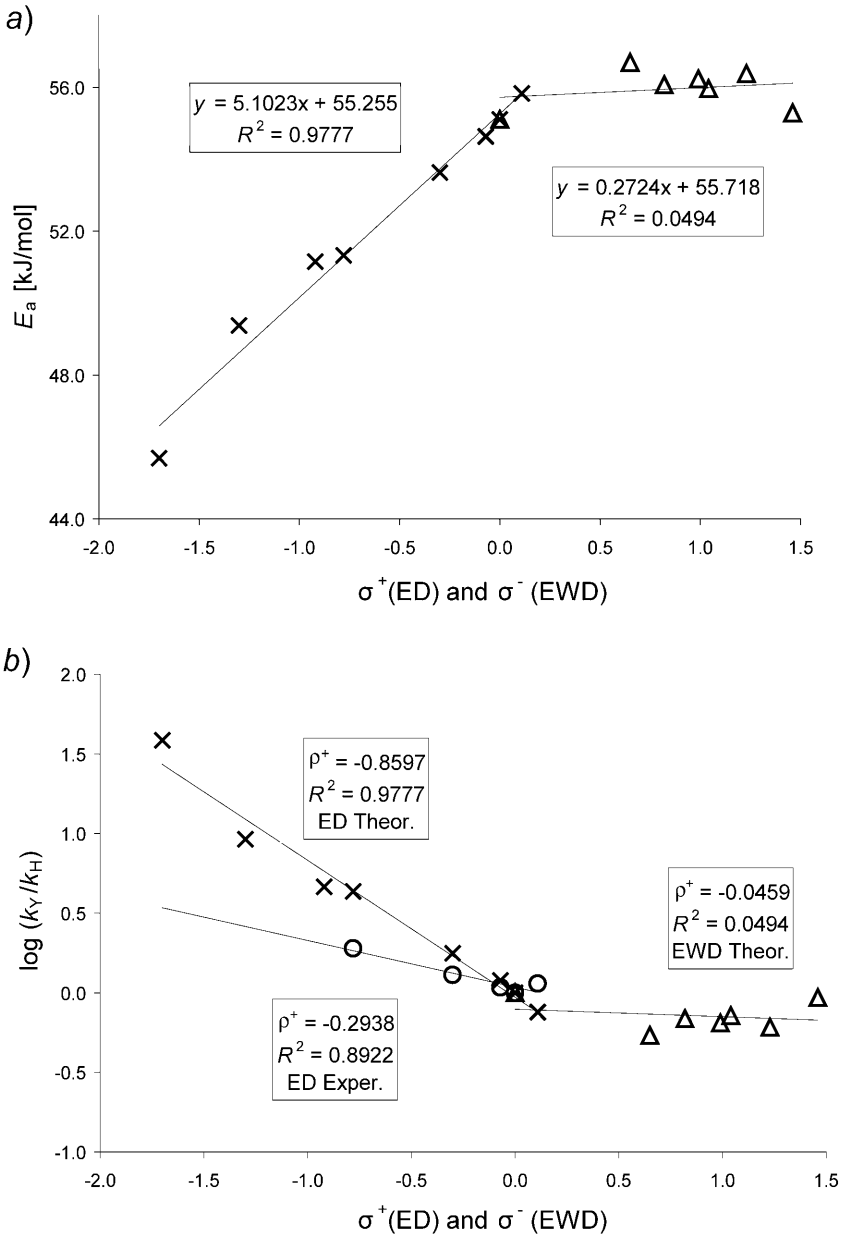

Fig. 2. a) *Plot of activation energy* (E_a) vs. Hammett *constants for substituted styrenes* (see *Scheme 1*). b) *Hammett plots for substituted styrenes.* Crosses (×) and triangles (△) refer to theoretical values, open circles (○) designate experimental values (see *Table 1*). $\varrho^+(\mathrm{ED}) = -0.86$ (-0.29 exper.); $\varrho^-(\mathrm{EWD}) = -0.05$, where ED and EWD refer to electron-donating and -withdrawing groups (by resonance), resp.

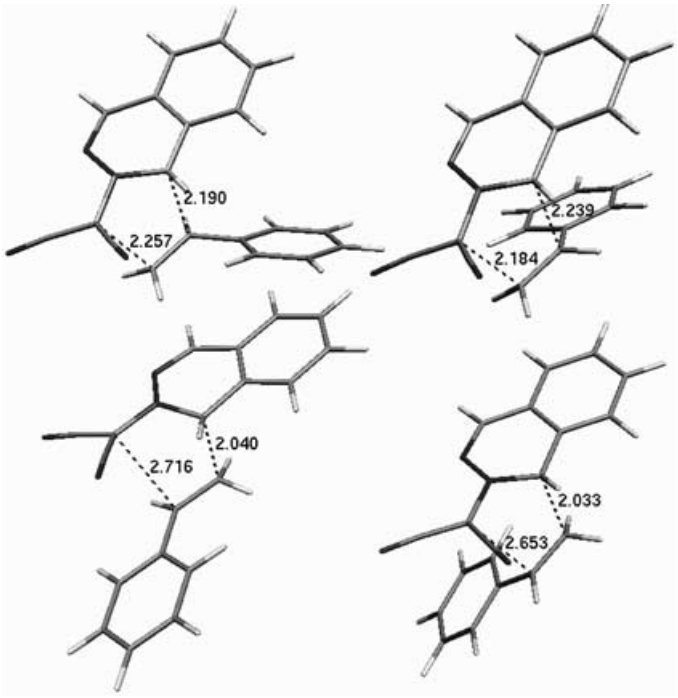

Fig. 3. *Calculated transtition-state structures for the reaction of* **1** *with styrene* (see *Scheme 1*). Distances of bonds to be formed are given in Å. Upper left: *exo*-**1**, upper right: *endo*-**1**, lower left: *exo*-**2**, lower right: *endo*-**1**.

A number of representative synthetic reactions were carried out with the styrene series separately in MeCN and H_2O to parallel the kinetics study (*Table 1*). In each case, the major product was the *exo*-configured regioisomer **3**. The analogous *endo*-isomer was a minor product. The difference was readily indicated in the ^{1}H-NMR spectra, where the signal for H–C(10b) appeared as a *dd* due to the adjacent CH_2(1) group. NOE Difference spectra confirmed the *exo*- and *endo*-configurations, the former of which was supported by an X-ray crystal-structure analysis of a similar electron-rich dipolarophile [3]. Only with a NO_2 group on the styrene phenyl ring did the reaction start to show the beginning of the changeover to the $HOMO_{dipole}$ mode, where a low yield of the reversed regio product appeared (*Table 1*, *Entry 8*). In this compound, the H–C(10b) ^{1}H-NMR signal is now a simple *d* due to the presence of a single H-atom only at C(1). *Although the reactants appeared visually insoluble in H_2O, the aqueous suspensions readily reacted over 24 h at 80°, and the* exo/endo *ratio was little altered by the H_2O environment, where a slight increase in preference for the* exo-*isomer was apparent* (*Table 1*). Normally, in *Diels–Alder* reactions with electron-poor dienophiles, H_2O tends to favour the *endo*-configured transition state.

2. '*Benzylidene Acetones*'[2]). In order to assess the effect of H_2O on the polarity of the transition state for the 'water-super' dipolarophile, the alkyl vinyl ketone structure,

[2]) Systematic name: 4-arylbut-3-en-2-ones.

we attempted to determine ρ values for the reactions of the benzylidene acetone series **4** with the 1,3-dipole **1**. The synthetic course of the *separate* reactions of **1** with MVK and styrenes is summarised in *Scheme 1*. When both of these structural features are included in a single dipolarophile **4**, the product **5** (and the minor adduct **6**) might be expected from transition states comparable to those by which **2** and **3** are formed (see *Scheme 2*). Calculated activation energies, however, predicted that the regiochemistry would be reversed. The experimental results showed the major product to be **7** (with **8** as a minor product) for the reactions of **1** with **4** (Y = H, Cl, Me) in MeCN.

Scheme 2

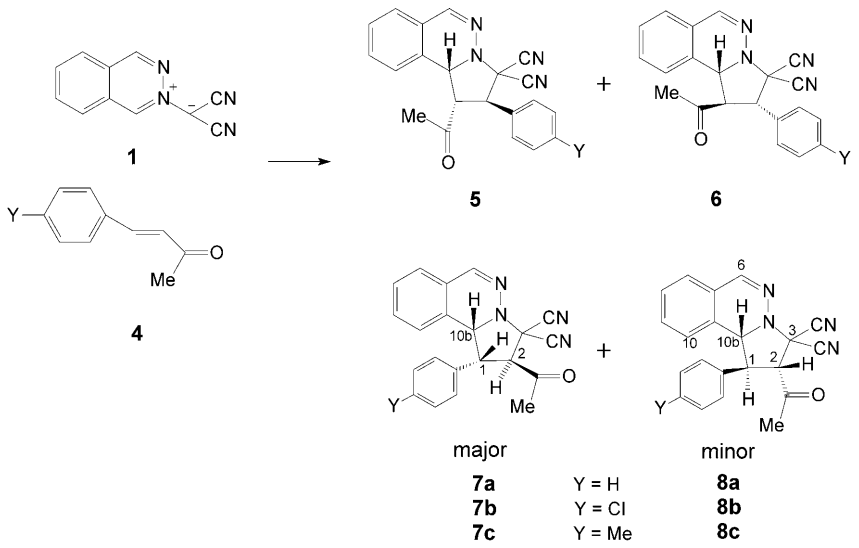

The structures of compounds **7** and **8** were confirmed by microanalyses, ^{1}H- and ^{13}C-NMR spectra (supported by COSY and DEPT spectra), and NOE difference spectra to determine configurations. In the products **7**, the ^{1}H-NMR spectrum showed H–C(10b) as a *d* at δ(H) 5.25, H–C(1) as a *dd* at 3.86–3.94, and H–C(2) as a *d* at 4.25–4.27. A strong NOE (12–14%) between H–C(10b) and H–C(1), and the absence of an NOE from each of these to H–C(2), indicated the aryl and the Ac substituents in *endo*- and *exo*-positions, respectively. In the minor products **8**, the *exo*-aryl group at C(1) caused shielding of the bridgehead H–C(10b) to δ(H) 4.6–4.7, and an NOE between H–C(2) and H–C(10b) (7–9%) supported this configuration. The ratio of **7**/**8** in the product mixture was *ca.* 10:1. No interconversion or changes in products took place under the reaction and workup conditions.

The second-order rate constants for the reactions of the dipole **1** with **4a** at 37° in MeCN *vs.* H_2O/MeCN 9:1 were 7.20×10^{-4} and 2.40×10^{-2} l mol^{-1}s^{-1}, respectively. This corresponds to a rate enhancement of 33.8 in the aqueous medium, and indicates that the 'water-super' dipolarophile nature of the vinyl ketone structure is still present in the dipolarophiles **4**. Theoretical calculations were carried out in the same manner for benzylidene acetones as for the styrenes. The same set of *para*-substituents were also used. *Fig. 4,a* illustrates the effect of these substituents on the activation energies. We

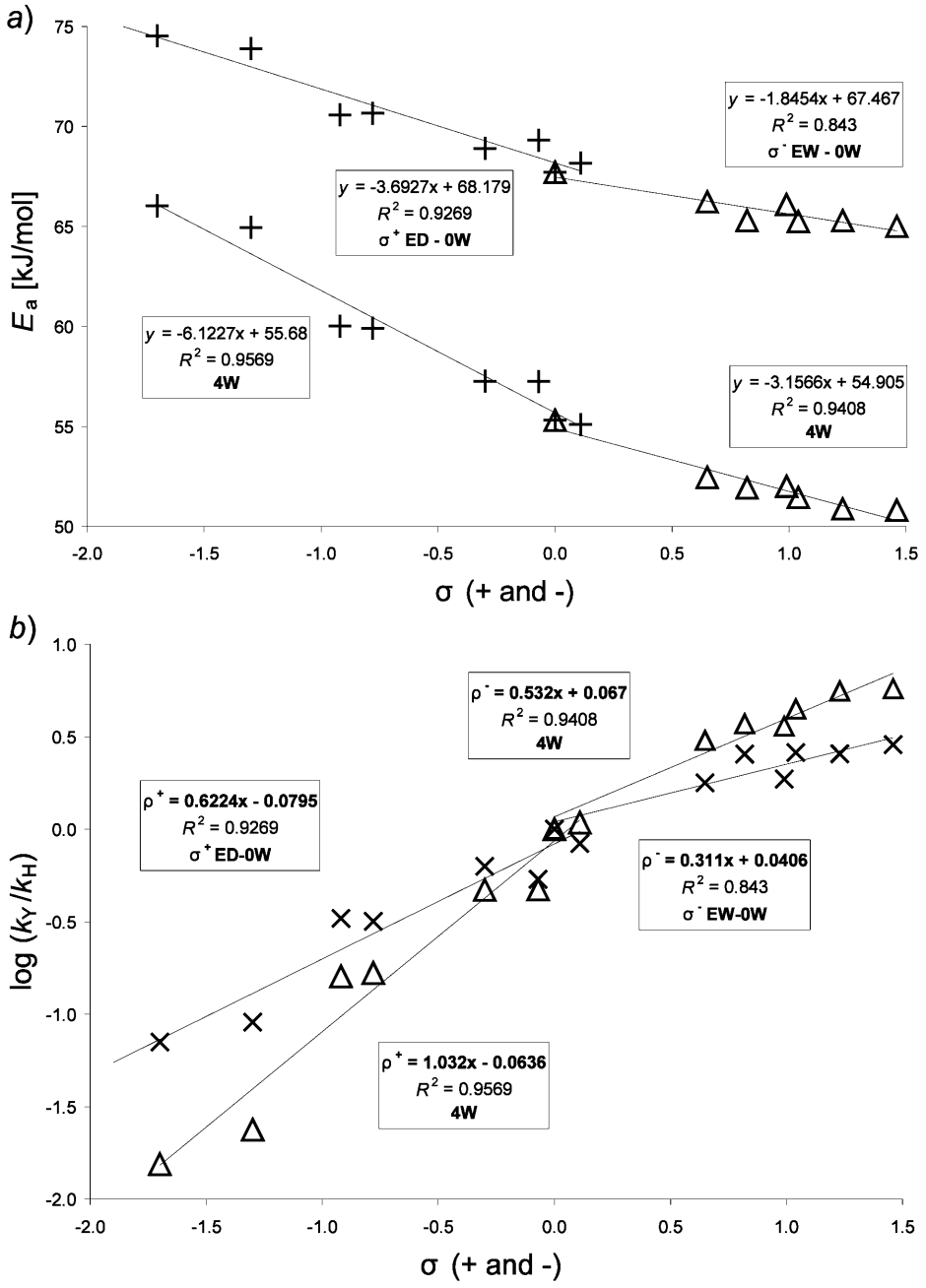

Fig. 4. a) *Plot of activation energy* (E_a) vs. Hammett *constants for compounds* **4** (as in *Table 2*). ED and EWD refer to electron-donating and -withdrawing groups (by resonance), resp.; and 0W and 4W refer to water clusters made of zero and four H_2O molecules, resp.). b) *Theoretical* Hammett *plots* for *compounds* **4**. Crosses (×) refer to 0W, triangles (△) to 4W conditions, resp. $\varrho^+(\mathrm{ED}-0\mathrm{W})=+0.62$; $\varrho^+(\mathrm{ED}-4\mathrm{W})=+1.03$; $\varrho^-(\mathrm{EW}-0\mathrm{W})=+0.31$; $\varrho^-(\mathrm{EW}-4\mathrm{W})=+0.53$.

found that the best correlation is achieved when the substituents are grouped into σ^+ and σ^--*Hammett* constants. Both groups give rise to a negative slope, but the ED groups give a larger absolute value. *Fig. 4, b* shows a *Hammett* plot. The ρ^+ value for ED groups is 0.62, and for EWD groups, ρ^- is 0.31.

Fig. 5 represents the transition-state structures for the four possible isomers. In referring to the isomers, we abbreviate the names by referring to the position of the ketone substituent, contrary to the styrene case. We do this because it is the 1,3-dipole that determines the regiochemistry, the lower-energy regioisomer being in every case the 2-keto isomer. As for the styrenes, the calculations do not reflect the relative *endo*/*exo* product ratios, and a solvophobic effect, which favours the *endo*-arrangement for the aryl substituent, may be operating.

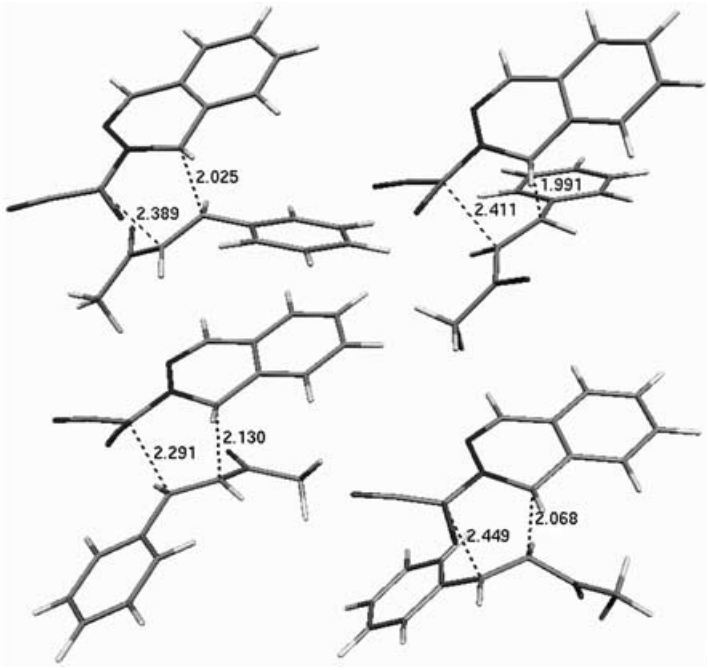

Fig. 5. *Calculated transtition-state structures for the reaction of* **1** *with* **4** (see *Schemes 2* and *3*). Distances of bonds to be formed are given in Å. Upper left: *endo*-**2**, upper right: *exo*-**2**, lower left: *endo*-**1**, lower right: *exo*-**1** (isomer takes its abbreviated name from the position of the keto substituent).

Calculations were repeated with a cluster of four H_2O molecules on the C=O O-atom of the benzylidene acetones and the transition-state structures. A H_2O dimer had first been chosen, but the optimisation procedures brought the dimer from a higher energy structure, where two H-atoms of the dimer were bonded to the C=O O-atom to another structure, in which the dimer fits in the notch between the C=O O-atom and the benzylidene CH group. This structure was not predominant in our previous study on MVK [5].

Theoretical calculations indicated the concerted transition state **9** (or **9a**) shown in *Scheme 3*, in which a key feature is the dipolar interaction along the developing

Scheme 3

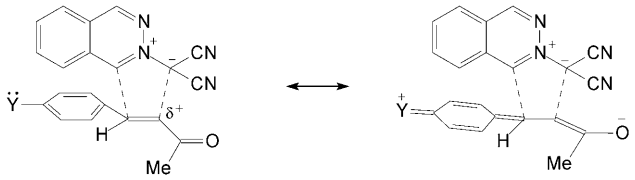

C(2)–C(3) bond. Strong resonance-electron-donating substituents inhibited the rate by reducing the positive charge at C(2) in the transition state (*Scheme 3*).

The calculated *Hammett* ρ^+ values, for H_2O clusters made of zero ($\rho^+ = 0.62$) and four molecules (1.03), do not suggest a significant increase in the polarity of the transition state in the presence of the H_2O cluster on the keto substituent. Although there is a clear rate enhancement in the presence of the cluster with four H_2O, it is

Table 3. *Theoretical Calculations for Substituted Benzylidene Acetones* (see *Scheme 2*). The terms '0W' and '4W' refer to clusters of zero and four H_2O molecules, resp. For symbols of physical quantities and their units, see *Table 2*.

Y	Keto position	0W				4W			
		E_a	$-S_a$	G_a	$\log(k_Y/k_H)$	E_a	$-S_a$	G_a	$\log(k_Y/k_H)$
H	2-*endo*	67.71	214.15	134.68	0.000	55.30	228.05	125.63	0.000
	1-*endo*	74.85	207.13	138.96					
	2-*exo*	73.34	204.40	136.64		62.81	215.20	129.42	
	1-*exo*	74.31	203.89	137.45					
Me_2N	2-*endo*	74.54	217.86	142.05	−1.151	66.04	233.26	137.93	−1.810
NH_2	2-*endo*	73.90	212.55	140.30	−1.043	64.95	229.07	135.37	−1.625
OH	2-*endo*	70.57	213.46	137.28	−0.483	60.02	229.02	130.50	−0.795
Me	2-*endo*	68.90	213.33	135.63	−0.201	57.25	225.15	129.23	−0.329
	1-*endo*	75.04	203.69	138.10					
	2-*exo*	74.06	211.16	139.63					
	1-*exo*	73.91	207.00	138.01					
MeO	2-*endo*	70.66	211.35	136.59	−0.498	59.91	229.36	130.79	−0.777
	1-*endo*	75.14	203.84	138.26					
	2-*exo*	75.17	207.99	139.82					
	1-*exo*	74.60	202.27	137.26					
F	2-*endo*	69.31	213.76	136.12	−0.270	57.25	227.47	127.33	−0.328
Cl	2-*endo*	68.16	210.78	133.91	−0.076	55.08	229.71	126.40	0.037
	1-*endo*	74.44	206.37	138.20					
	2-*exo*	72.98	207.84	137.50					
	1-*exo*	74.08	204.79	137.61					
CHO	2-*endo*	65.25	212.81	131.61	0.415	51.45	231.81	123.63	0.650
Ac	2-*endo*	65.30	212.77	131.86	0.406	51.92	230.75	123.77	0.570
CF_3	2-*endo*	66.22	215.27	133.33	0.251	52.45	235.73	125.54	0.480
CN	2-*endo*	66.09	213.30	132.65	0.272	52.00	231.32	123.94	0.556
NO	2-*endo*	64.99	212.28	131.20	0.458	50.80	232.45	123.32	0.759
NO_2	2-*endo*	65.29	209.81	130.79	0.408	50.87	230.88	122.79	0.747
	1-*endo*	71.98	207.74	136.18					
	2-*exo*	70.25	208.23	135.04					
	1-*exo*	70.77	207.38	135.1					

remarkable that the spread of the individual points on the graph (*Fig. 4,a*) is paralleled with and without H_2O. The calculated values are summarised in *Table 3*.

A Personal Anecdote[3]). – I first met *Rolf* and *Trudl Huisgen* in July 1990, when they visited Galway for a Euchem Conference on 1,3-dipolar cycloaddition reactions. A family friendship developed, where *Trudl* and my wife *Jean* found much to share among the traditions of Bavaria and Connemara. Following that meeting, *Rolf* and I engaged in continuing contact on chemistry matters, in which his deep insight and enthusiasm proved to be inspirational. Among the abiding effects from my point of view were his encouragement of our work on pentazoles, his views and approaches to teaching of frontier-orbital theory to undergraduate students, and a shared exchange of publications. My work in the early 1990s was focused on some interesting multi-step reactions of 1,3-dipoles embedded in azole rings. One of these reactions involved an easy *in situ* thermal 1,4-sigmatropic rearrangement in a cycloadduct. Since thermal sigmatropic rearrangements allowed by *Woodward–Hofmann* HOMO symmetry should proceed in a 1,5-manner, the 1,4-case required some consideration. *Rolf Huisgen* had highlighted symmetry-allowed photochemical 1,4-rearrangements in his landmark review [18] of electrocyclisations. Thus, when I raised the question of the thermal analogue with him, he took an exceptional interest. Following written discussions and exchanges, we drafted a note on thermal hetero-1,4-cyclisations, which we discussed in Munich in 1996. The draft manuscript, as it was in August 1996, is included herein in the *Appendix*; a theoretical comment has been added by Professor *Luke Burke*. Shortly after this, I was unexpectedly struck by a health problem similar to that which caused the premature loss [19] of my friend *Gerrit L'abbé* (who also delivered a plenary lecture at the Galway Euchem Conference). For me, the long recovery to resume normal teaching and administrative duties put an end to much ongoing academic research at the time, including the 1,4-sigmatropic rearrangement.

One of my most-abiding experiences with *Rolf Huisgen* was a never-to-be-forgotten tour of the Munich Alte and Neue Pinakothek. I know that others, who have been similarly privileged, have been equally astounded by this remarkable scholar of chemistry and art. In a report [20] to the Institute of Chemistry of Ireland on the Euchem conference, I finished as follows:

> *Throughout the conference the World Cup became a major cause for administrative improvisation with England, Italy and West Germany featuring in the semi-finals on the Tuesday and Wednesday evenings.* Rolf Huisgen *had little interest in this but he seemed intrigued with the necessity which arose for the organisers to make sure that the international participants were able to see the matches during the social events. He gave a closing address at the end of the conference in which he stated 'we cannot ignore the world around us' – comments on the violence then being experienced at world cup matches – 'let me compare the world of sport with the world of science. How peaceful is the world of science. We do not score goals against one another. We work together to increase knowledge'. This gives a telling insight into the intellect of one of the finest scholars of chemistry.'*

Alles Leben, tief gelebt,
ist ein Gebet,
ist ein Gesang, darinnen schwebt,
was schnell vergeht –
und bleibt im tiefsten Grunde doch.
Die Blume sieh,
sie haucht es im Verwelken noch:
für immer nie!

Klaus Huisgen, 1943[4])

---

[3]) By *Richard N. Butler*.

[4]) A poem by *Rolf*'s brother *Klaus* (1917–1944); interpreted (inadequately) by *R. N. B.*:

Every life, heartfeltly lived,
is a prayer,
and holds within a song,
that quickly vanishes –
and yet surely doth persist in deepest core.
The flower that breathes within it
does not fade:
ever!

L. A. B. acknowledges the *National Science Foundation* for a computer-equipment grant (MRI 9871088). *E. M. M.* acknowledges support from the *Irish Research Council for Science, Engineering and Technology.*

Experimental Part

1. *General. Dicyano(phthalazin-2-ium-2-yl)methanide* (**1**) was prepared according to known procedures [3]. Melting points (m.p.) were measured on an electrothermal apparatus; uncorrected. IR Spectra (nujol): *Perkin-Elmer Spectrum-1000* spectrophotometer; in cm^{-1}. NMR Spectra: *JEOL GXFT-400* instrument; in $CDCl_3$ or $(D_6)DMSO$, δ rel. to Me_4Si as internal reference, J in Hz; assignments supported by selective H-decoupling, COSY, DEPT, and NOEDS experiments. Microanalyses were determined on a *Perkin-Elmer-240 CHN Analyser*.

2. *Reactions of* **1** *with Substituted Styrenes.* 2.1. *In MeCN. General Procedure* (*GP 1*): A suspension of **1** (1.54 mmol) in MeCN (20 ml) was treated with the appropriate styrene (3.08 mmol), and stirred under reflux for 24 h. Then, the solvent was removed under reduced pressure, the residue was dissolved in CH_2Cl_2 (4 ml), and subjected to flash chromatography (FC) (SiO_2, ASTM 230–400 mesh; CH_2Cl_2/petroleum ether (PE; b.p. 40–60°) 1:1 → 1:0 in 2.5% (*v*/*v*) gradient steps).

2.2. *In Water. General Procedure* (*GP 2*) [21]: A suspension of **1** (1.54 mmol) in H_2O (20 ml) was treated with the appropriate styrene (3.08 mmol), and stirred at 80° for 24 h. The mixture was allowed to cool down, the products were extracted with CH_2Cl_2 (2 × 10 ml), and the combined org. layer was dried ($MgSO_4$) and evaporated under reduced pressure. The resulting residue was subjected to FC as described in *GP 1*.

2-exo-*1,2,3,10b-Tetrahydro-2-phenylpyrrolo[2,1-*a*]phthalazine-3,3-dicarbonitrile* (*exo*-**3a**). Yield: 74%. Colorless solid. M.p. 158–160° (EtOH). IR: 666, 759 (Ph). ^{1}H-NMR ($CDCl_3$): 2.74–2.85 (*m*, CH_2(1)); 4.15 (*dd*, *J* = 10.7, 7.3, H–C(2)); 4.52 (*dd*, *J* = 8.8, 8.5, H–C(10b)); 7.18 (*d*, *J* = 7.3, H–C(10)); 7.25–7.54 (*m*, H–C(7,8,9), Ph); 7.80 (*s*, H–C(6)). ^{13}C-NMR ($CDCl_3$): 29.7 (C(1)); 52.2 (C(2)); 56.3 (C(10b)); 63.7 (C(3)); 110.8, 113.3 (CN); 123.1 (C(10)); 125.1 (C(10a)); 126.0 (C(9)); 128.7, 129.2, 134.7 (Ph); 129.4 (C(8)); 132.0 (C(7)); 133.7 (C(6a)); 146.5 (C(6)); the resonance for C(4′) was masked by that of C(3′). Anal. calc. for $C_{19}H_{14}N_4$ (298.34): C 76.5, H 4.7, N 18.7; found: C 76.2, H 4.4, N 18.5.

2-endo-*1,2,3,10b-Tetrahydro-2-phenylpyrrolo[2,1-*a*]phthalazine-3,3-dicarbonitrile* (*endo*-**3a**) Yield: 13%. Eluted after *exo*-**3a**. Gum. ^{1}H-NMR ($CDCl_3$): 2.56–2.64 (*m*, H_{endo}–C(1)); 2.99–3.03 (*m*, H_{exo}–C(1)); 4.18 (*dd*, *J* = 8.8, 8.3, H–C(2)); 4.54 (*dd*, *J* = 10.2, 5.8, H–C(10b)); 7.13–7.57 (*m*, H–C(7,8,9,10), Ph); 7.78 (*s*, H–C(6)). ^{13}C-NMR ($CDCl_3$): 33.5 (C(1)); 53.2 (C(2)); 56.3 (C(10b)); 111.7, 113.2 (CN); 122.9 (C(10)); 128.7, 129.2, 136.7 (C(1′), C(2′), C(3′)); 124.2, 129.0, 132.2 (C(7) to C(10)); 145.9 (C(6)); the signal for C(3) was too weak to be observed with the small quantity available.

2-exo-*1,2,3,10b-Tetrahydro-2-(4-methoxyphenyl)pyrrolo[2,1-*a*]phthalazine-3,3-dicarbonitrile* (*exo*-**3b**). Yield: 63%. Colorless solid. M.p. 159–162° (EtOH). IR: 831 (C_6H_4), 1036, 1260 (C–O–C), 2213 (CN). ^{1}H-NMR ($CDCl_3$): 2.69–2.87 (*m*, CH_2(1)); 3.85 (*s*, MeO); 4.13(*dd*, *J* = 11.3, 6.8, H–C(2)); 4.52 (*dd*, *J* = 8.7, 8.3, H–C(10b)); 6.98–7.77 (*m*, H–C(7,8,9,10), H–C(2′,3′)); 7.80 (*s*, H–C(6)). ^{13}C-NMR ($CDCl_3$): 29.8 (C(1)); 51.7 (C(2)); 55.3 (MeO); 56.3 (C(10b)); 63.5 (C(3)); 111.0, 113.5 (CN); 114.6 (C(3′)); 123.4 (C(10)); 125.0 (C(10a)); 125.5 (C(1′)); 126.0 (C(9)); 128.5 (C(8)); 129.9 (C(2′)); 132.0 (C(7)); 134.7 (C(6a)); 146.4 (C(6)); 160.3 (C(4′)). Anal. calc. for $C_{20}H_{16}N_4O$ (328.36): C 73.15, H 4.9, N 17.1; found: C 72.8, H 4.5, N 17.2.

2-endo-*1,2,3,10b-Tetrahydro-2-(4-methoxyphenyl)pyrrolo[2,1-*a*]phthalazine-3,3-dicarbonitrile* (*endo*-**3b**). Yield: 8%. Eluted after *exo*-**3b**. Gum. ^{1}H-NMR ($CDCl_3$): 2.54–2.59 (*m*, H_{endo}–C(1)); 2.97–2.99 (*m*, H_{exo}–C(1)); 3.79 (s, MeO); 4.15 (*dd*, *J* = 8.8, 8.3, H–C(2)); 4.54 (*dd*, H–C(10b)); 6.90 (*d*, *J* = 8.8, H–C(10)); 7.12–7.50 (*m*, H–C(7,8,9), H–C(2′,3′)); 7.75 (*s*, H–C(6)).

2-exo-*2-(3-Fluorophenyl)-1,2,3,10b-tetrahydropyrrolo[2,1-*a*]phthalazine-3,3-dicarbonitrile* (*exo*-**3e**). Yield: 76%. Colorless solid. M.p. 152–154° (EtOH). IR: 774 (*o*-disubstituted benzene), 2146 (CN). ^{1}H-NMR ($CDCl_3$): 2.71–2.79 (*m*, H_{exo}–C(1)); 2.82–2.90 (*m*, H_{endo}–C(1)); 4.17 (*dd*, *J* = 11.2, 6.8, H–C(2)); 4.54 (*t*-like *dd*, *J* = 8.8, 8.8, H–C(10b)); 7.13–7.55 (*m*, H–C(7,8,9,10), H–C(2′,4′,5′,6′)); 7.81 (*s*, H–C(6)). ^{13}C-NMR ($CDCl_3$): 29.6 (C(1)); 51.7 (C(2)); 56.1 (C(10b)); 63.0 (C(3)); 110.6, 113.1 (CN); 115.7 (*d*, *J*(F,C) = 22.5, C(2′) or C(4′)); 116.5 (*d*, *J*(F,C) = 18.2, C(4′) or C(2′)); 123.1 (C(10a)); 124.5 (C(10)); 126.1 (C(6′)); 128.7 (C(9), C(5′)); 130.9 (C(8)); 132.0 (C(7)); 136.0 (C(1′)); 136.1 (C(6a)); 146.6 (C(6)); 163.0 (*d*, *J*(F,C) = 143.1, C(3′)). Anal. calc. for $C_{19}H_{13}FN_4$ (316.33): C 72.1, H 4.1, N 17.7; found: C 71.8, H 4.1, N 18.0.

2-endo-*2-(3-Fluorophenyl)-1,2,3,10b-tetrahydropyrrolo[2,1-*a*]phthalazine-3,3-dicarbonitrile* (*endo*-**3e**). Yield: 15%. Eluted together with *exo*-**3e**. ^{1}H-NMR ($CDCl_3$): 2.49–2.53 (*m*, H_{endo}–C(1)); 2.99–3.02 (*m*,

H_{exo}–C(1)); 7.03–7.67 (*m*, H–C(7,8,9,10), H–C(2′,4′,5′,6′)); 7.71 (*s*, H–C(6)); the resonances for H–C(8a) and H–C(2) were masked by those for H–C(8a) and H–C(2), resp., of the main isomer in the mixture.

2-exo-*1,2,3,10b-Tetrahydro-2-(3-nitrophenyl)pyrrolo[2,1-*a*]phthalazine-3,3-dicarbonitrile* (*exo*-**3h**). Yield: 68%. Colorless solid. M.p. 235–238° (EtOH). IR: 763 (*o*-disubstituted benzene). ^{1}H-NMR ((D$_6$)DMSO): 2.79–2.88 (*m*, H_{endo}–C(1)); 2.96–3.03 (*m*, H_{exo}–C(1)); 4.58 (*dd*, *J* = 8.8, 8.3, H–C(10b)); 4.86 (*dd*, *J* = 11.2, 5.8, H–C(2)); 7.36 (*d*, *J* = 7.3, H–C(10)); 7.49–7.64 (*m*, H–C(7,8,9)); 7.86 (*dd*, *J* = 8.3, 7.8, H–C(5′)); 8.07 (*s*, H–C(6)); 8.14 (*d*, *J* = 7.8, H–C(6′)); 8.35 (*d*, *J* = 8.3, H–C(4′)); 8.50 (*s*, H–C(2′)). ^{13}C-NMR ((D$_6$)DMSO): 29.1 (C(1)); 49.9 (C(2)); 56.5 (C(10b)); 63.0 (C(3)); 111.4, 113.5 (CN); 123.8 (C(10)); 124.2 (C(10a)); 126.3 (C(9)); 128.6 (C(8)); 130.8 (C(7)); 132.4 (C(6a)); 124.6, 135.8, 137.2 (C(1′,2′,4′,5′,6′)); 147.3 (C(6)); 148.0 (C(3′)). Anal. calc. for $C_{19}H_{13}N_5O_2$ (343.33): C 66.5, H 3.8, N 20.4; found: C 66.6, H 3.9, N 20.6.

2-endo-*1,2,3,10b-Tetrahydro-2-(3-nitrophenyl)pyrrolo[2,1-*a*]phthalazine-3,3-dicarbonitrile* (*endo*-**3h**). Yield: 11%. Eluted together with an 1-aryl regiosiomeric side product (see below) after *exo*-**3h**. ^{1}H-NMR ($CDCl_3$): 2.54–2.61 (*m*, H_{endo}–C(1)); 3.11–3.18 (*m*, H_{exo}–C(1)); 4.32 (*dd*, *J* = 8.3, 8.3, H–C(2)); 4.58 (*dd*, *J* = 9.3, 3.3, H–C(10b)); 7.13–8.08 (*m*, H–C(7,8,9,10), H–C(2′,4′,5′,6′); 8.23 (*s*, H–C(6)).

2-endo-*1,2,3,10b-Tetrahydro-1-(3-nitrorophenyl)pyrrolo[2,1-*a*]phthalazine-3,3-dicarbonitrile.* Yield: 6%. ^{1}H-NMR ($CDCl_3$): 2.82 (*dd*, *J* = 14.6, 2.9, H_{endo}–C(2)); 3.51 (*dd*, *J* = 14.6, 9.3, H_{exo}–C(2)); 4.12 (*m*, H–C(1)); 4.90 (*d*, *J* = 6.3, H–C(10b)); 6.48 (*d*, *J* = 7.8, H–C(10)); 7.13–8.08 (*m*, H–C(7,8,9), H–C(2′,4′,5′,6′)); 8.27 (*s*, H–C(6)).

3. *Reactions of* **1** *with Substituted 'Benzylidene Acetones' in MeCN. General Procedure* (*GP 3*): A suspension of **1** (1.54 mmol) in MeCN (20 ml) was treated with **4** (4.62 mmol), and stirred under reflux for 4 h. Then, the solvent was removed under reduced pressure, and the residue was taken up in ice-cold Et_2O, which caused the major product to separate as a yellow solid. The ethereal filtrate contained further **7**, the minor product **8**, excess **4**, unreacted **1**, and some intractable gum. ^{1}H-NMR analysis of this mixture, combined with separation by FC (as described for *GP 1*) afforded the reported products **7**.

1-endo-*2*-exo-*2-Acetyl-1,2,3,10b-tetrahydro-1-phenylpyrrolo[2,1-*a*]phthalazine-3,3-dicarbonitrile* (**7a**). Yield: 60%. Yellow solid. M.p. 174–176° (EtOH). IR: 694, 770 (Ph), 1720 (C=O). ^{1}H-NMR ($CDCl_3$): 1.91 (*s*, Me); 3.94 (*dd*, *J* = 8.7. 7.8, H–C(1)); 4.27 (*d*, *J* = 7.8, H–C(2)); 5.24 (*d*, *J* = 8.7, H–C(10b)); 7.19 (*d*, *J* = 7.3, H–C(10)); 7.34 (*d*, *J* = 7.3, H–C(7)); 7.40–7.53 (*m*, H–C(8,9), Ph); 7.64 (*s*, H–C(6)). ^{13}C-NMR ($CDCl_3$): 31.4 (Me); 57.6 (C(10b)); 58.5, 59.4 (C(1), C(2)); 65.8 (C(3)); 111.3, 112.2 (CN); 124.5 (C(10a)); 126.0 (C(10)); 127.4 (C(9)); 128.8 (C(2′)); 129.6 (C(3′)); 129.8 (C(4′)); 129.9 (C(8)); 131.9 (C(6a)); 132.0 (C(7)); 144.6 (C(6)); 204.8 (C=0); the signal for C(1′) was masked. Anal. calc. for $C_{21}H_{16}N_4O$ (340.38): C 74.1, H 4.75, N 16.45; found: C 73.6, H 4.7, N 16.1.

1-exo-*2*-endo-*2-Acetyl-1,2,3,10b-tetrahydro-1-phenylpyrrolo[2,1-*a*]phthalazine-3,3-dicarbonitrile* (**8a**). Yield: 6%. ^{1}H-NMR ($CDCl_3$; mixture with **7a**; key signals): 3.80 (*dd*, H–C(1)); 4.21 (*J* = 7.3, H–C(2)); 4.64 (*d*, *J* = 8.7, H–C(10b)).

1-endo-*2*-exo-*2-Acetyl-1-(4-chlorophenyl)-1,2,3,10b-tetrahydropyrrolo[2,1-*a*]phthalazine-3,3-dicarbonitrile* (**7b**). Yield: 52%. Colorless solid. M.p. 162–163° (EtOH). IR: 761 (C–Cl) 1725 (C=O). ^{1}H-NMR ($CDCl_3$): 1.87 (*s*, Me); 3.86 (*dd*, H–C(1)); 4.26 (*d*, *J* = 7.8, H–C(2)); 5.25 (*d*, *J* = 7.3, H–C(10b)); 7.21 (*d*, *J* = 7.3, H–C(10)); 7.34 (*d*, *J* = 7.3, H–C(7)); 7.41–7.47 (*m*, H–C(8,9), H–C(2′,3′)); 7.63 (*s*, H–C(6)). ^{13}C-NMR ($CDCl_3$): 31.6 (Me); 57.2 (C(10b)); 58.9, 59.4 (C(1), C(2)); 65.9 (C(3)); 111.2, 111.9 (CN); 124.3 (C(10a)); 126.2 (C10); 127.5 (C(9)); 129.3 (C(1′)); 129.8 (C(2′)); 129.9 (C(8)); 130.1 (C(3′)); 130.4 (C(6a)); 132.1 (C(7)); 136.1 (C(4′)); 144.6 (C(6)); 204.5 (C=O). Anal. calc. for $C_{21}H_{15}ClN_4O$ (374.82): C 67.30, H 4.05, N 14.90; found: C 67.0, H 3.9, N 15.4.

1-exo-*2*-endo-*2-Acetyl-1-(4-chlorophenyl)-1,2,3,10b-tetrahydropyrrolo[2,1-*a*]phthalazine-3,3-dicarbonitrile* (**8b**). Yield: 5%. ^{1}H-NMR ($CDCl_3$; mixture with **7b**; key signals): 3.67 (*dd*, H–C(1)); 4.19 (*J* = 7.3, H–C(2)); 4.66 (*d*, *J* = 8.7, H–C(10b)).

1-endo-*2*-exo-*2-Acetyl-1,2,3,10b-tetrahydro-1-(4-methylphenyl)pyrrolo[2,1-*a*]phthalazine-3,3-dicarbonitrile* (**7c**). Yield: 69%. Yellow solid. M.p. 175–176° (EtOH). IR: 1725 (C=O). ^{1}H-NMR ($CDCl_3$) 1.92 (*s*, Ac); 2.37 (*s*, Me); 3.93 (*dd*, H–C(1)); 4.23 (*d*, *J* = 7.8, H–C(2)); 5.22 (*d*, *J* = 8.9, H–C(1)); 7.18 (*d*, *J* = 6.9, H–C(10)); 7.26 (*d*, *J* = 7.8, H–C(3′,5′)); 7.34 (*d*, *J* = 7.1, H–C(7)); 7.39–7.46 (*m*, H–C(8,9,2′,6′)); 7.64 (*s*, H–C(6)). ^{13}C-NMR ($CDCl_3$): 21.3 (Me); 31.3 (*Me*CO); 57.3 (C(10b)); 58.4, 59.3 (C(1), C(2)); 65.3 (C(3)); 111.3, 112.3 (CN); 124.5 (C(10a)); 125.9 (C(10)); 127.4 (C(9)); 128.7 (C(2′)); 128.9 (C(1′)); 129.7 (C(8)); 130.0 (C(6a)); 130.3 (C(3′)); 132.0 (C(7)); 140.0 (C(4′)); 144.6 (C(6)); 204.9 (C=O). Anal. calc. for $C_{22}H_{18}N_4O$ (354.40): C 74.55, H 5.1, N 15.8; found: C 74.4, H 4.8, N 15.85.

1-exo-*2*-endo-*2-Acetyl-1,2,3,10b-tetrahydro-1-(4-methylphenyl)pyrrolo[2,1-*a*]phthalazine-3,3-dicarbonitrile* (**8c**). Yield: 7%. ^{1}H-NMR ($CDCl_3$; mixture with **7c**; key signals): 3.69 (*dd*, H–C(1)); 4.11 ($J = 7.3$, 1 H, H–C(2)); 4.63 (*d*, $J = 9.2$, 1 H, H–C(10b)).

4. *Determination of Reaction Rates.* The rate constants k were determined by UV/VIS spectroscopy, monitoring the disappearance of **1** at 411 nm (λ_{max}). A *Hewlett-Packard Agilent Technologies 8453* spectrophotometer was used, featuring an automatic changer for up to eight glass cuvettes of 1-cm path length. The temp. was maintained constant within $\pm 0.2°$ by means of a thermostat (*Haake DC10*; water bath), with a separate calibrated thermometer check. The reactions were monitored under pseudo-first-order conditions. The initial concentration of **1** was 3.2×10^{-5} M, and a 50- to 10000-fold excess of dipolarophile was used. Kinetic runs were preformed at three different concentrations of dipolarophiles, and repeated at least three times. The allowed reaction times ranged from 1–15 h (styrenes), and from 1–4 d (benzylidene acetones), depending on the dipolarophile and condition. The soln. changed from yellow to colourless, as the reaction progressed.

In a typical kinetic run, first the dipole soln. (2 ml) was placed in a tightly capped cuvette (1 cm) and left to equilibrate at a given temp. for 10 min. The dipolarophile soln. (1 ml) was then added, the mixture was shaken and allowed to equilibrate, before the absorbance (A) was measured. A plot of $\ln(A_t - A_\infty)$ *vs.* time t for more than 3 half-lives gave a line whose slope corresponds the pseudo-first-order rate constant. These lines typically gave r values of ≥ 0.999. Plots of the measured pseudo-first-order rate constants, with the origin as an extra point, *vs.* the molarity of the dipolarophile, gave lines ($r \geq 0.993$), with slopes corresponding to the second-order rate constants quoted. All second-order rate constants were determined at least three times, and were reproducible to $\pm 2.5\%$ (styrenes) and $\pm 5.0\%$ (benzylidene acetones).

Appendix

Here, we present the uncompleted (editorially adapted) draft of a manuscript written by *Rolf Huisgen* and *Richard N. Butler* in 1996. Title: *Allowed Suprafacial Thermal 1,4-Sigmatropic Rearrangement of Conjugated Organic Nitrogen Systems: Analogue of the 1,5-Sigmatropic Rearrangement of Carbon Systems: A Comment.*

In recent studies of the reactions of exocyclic azolium ylide 1,3-dipoles, where two of the four π-electrons of the 1,3-dipole are embedded in a higher azole ring, a general sequence of a cycloaddition, followed by rearrangement, has been observed (*Scheme A1*)[1–3]. With these systems, the rearrangement of **A1** invariably involves an easy suprafacial, symmetry-allowed 1,4-sigmatropic migration to **A2**, which occurs *in situ*. We wish to briefly point out that such a 1,4-sigmatropic migration is a natural N-analogue of the well-known 1,5-sigmatropic rearrangement of the 1,3-diene system (**A3** → **A4** *vs.* **A5** → **A6**; *Scheme A2*), and that it should be widespread in organic N-systems. The difference from the C-analogue is that, for the N-case, the four π-electrons may be delocalised over three atoms, thus causing a 1,4-shift rather than the 1,5-migration, which occurs when these electrons are delocalised on four atoms, as in a diene. Why are these shifts apparently so rare in the literature? It is likely that, as shown in *Scheme A1*, they occur mainly in short-lived intermediates and, hence, are not as strikingly evident as the well-known 1,5-C shifts in stable precursors.

Scheme A1

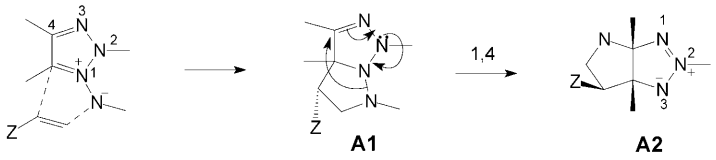

Possibly the best-known example of an N-containing 1,4-sigmatropic shift is the *Sommelet–Hauser* rearrangement (*Scheme A3*)[4–8]. This reaction, which could be looked on as an allylic *Stevens* rearrangement, has not been classified in the context of its relationship with the 1,5-C sigmatropic shift. A new example of it, the conversion **A7** → **A9**, has recently been reported[9] (*Scheme A4*).

Scheme A2

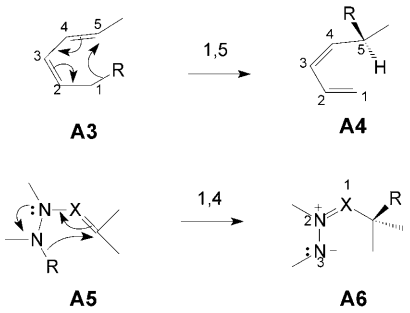

Scheme A3

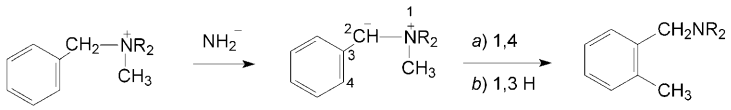

Scheme A4

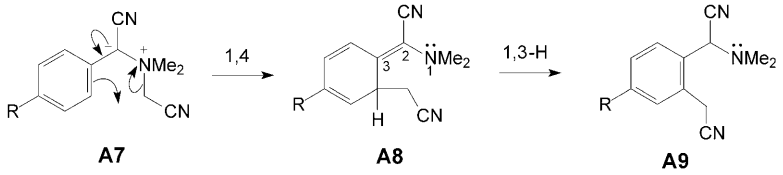

Another case where a 1,4-shift appears to be significant is in the ring contraction and rearrangement of unstable tetra-azocines, **A10**, which rearrange to **A11**[10] (*Scheme A5*). A 1,4-alkyl migration has recently been reported[11] at 200° in the 1-alkoxytetrazole system **A12**, which rearranges to **A13** (*Scheme A5*). Although this reaction was shown to be intermolecular at these high temperatures by detection of crossover products, the possibility that some of it followed an intramolecular path appears not to be excluded at present. 1,4-H Migrations, *e.g.*, **A14** → **A15** (*Scheme A5*), are an accompanying feature of many 1,3-dipolar cycloadditions[12], and these are N-analogues of the ubiquitous 1,5-H-shifts of diene systems. The thermal 1,4-rearrangements are most-easily recognised by the distribution of the four π-electrons over the three atoms in positions 1, 2, and 3 in the products. Many more examples of this type of rearrangement should be expected.

The feasibility of the 1,4-heterosigmatropic rearrangement is indicated by ongoing calculations by *L. A. Burke* on molecules **A14** and A**15** with H-atoms as substituents, using the commonly accepted B3LYP/6-31G(d) theoretical method (2005). The ΔE values were calculated to be -25.7 kcal mol^{-1} for the isomerisation of the 1,3-dipole **A14** to **A15**, a molecule with a 'conventional' *Lewis* structure. The activation energy, E_a, starting from **A14**, amounts to 34.4 kcal mol^{-1}. This value lies within the values commonly found for 'allowed' pericyclic reactions. In *Fig. A*, structural representations of **A14** and **A15**, and of the corresponding transition state, are shown. The distances (in Å) indicated in the transition state reflect the difference in energy of the reactant dipole **A14** and the product **A15**. The transition-state structure resembles more the higher-energy dipole than the product.

Scheme A5

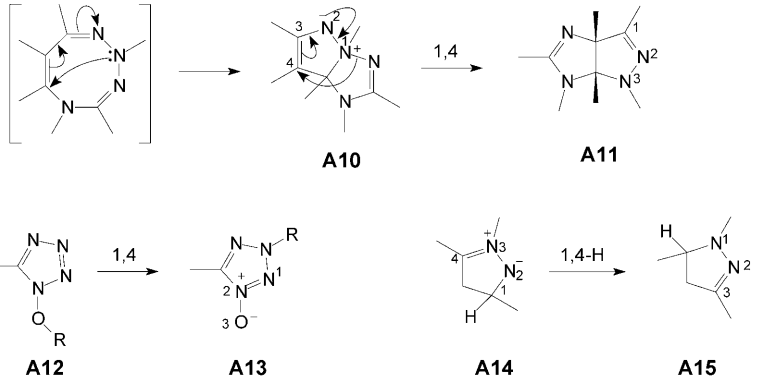

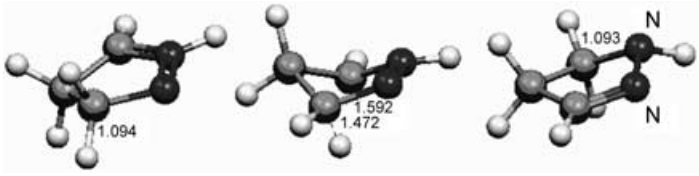

Fig. A. *Structures of* **A14** (left) *and* **A15** (right), *together with the corresponding transition-state structure* (center). See *Scheme A5*. Bond lengths in Å.

[1] R. N. Butler, A. M. Evans, A. M. Gillan, J. P. James, E. McNeela, D. Cunningham, P. McArdle, *J. Chem. Soc.*, *Perkin Trans. 1* **1990**, 2537.
[2] R. N. Butler, A. M. Evans, E. McNeela, G. A. O'Halloran, P. D. O'Shea, D. Cunningham, P. McArdle, *J. Chem. Soc.*, *Perkin Trans. 1* **1990**, 2527.
[3] R. N. Butler, F. A. Lysaght, L. A. Burke, *J. Chem. Soc.*, *Perkin Trans. 2* **1992**, 1103.
[4] S. W. Kantor, C. R. Hauser, *J. Am. Chem. Soc*. **1951**, *73*, 4122.
[5] G. C. Jones, C. R. Hauser, *J. Org. Chem.* **1962**, *27*, 3572.
[6] C. R. Hauser, A. J. Weinheimer, *J. Am. Chem. Soc.* **1954**, *76*, 1264.
[7] W. Q. Beard Jr., C. R. Hauser, *J. Org. Chem*. **1960**, *25*, 334.
[8] J. Biellmann, J. Schmitt, *Tetrahedron Lett.* **1973**, 4615.
[9] T. Zdojewski, A. Jończyk, *Tetrahedron Lett.* **1995**, *36*, 1355.
[10] R. N. Butler, D. M. Colleran, D. F. O'Shea, D. Cunningham, P. McArdle, A. M. Gillan, *J. Chem. Soc.*, *Perkin Trans. 1* **1993**, 2757.
[11] J. Plenkiewicz, A. Roszkiewicz, *Pol. J. Chem.* **1993**, *67*, 1767.
[12] H. Gotthardt, R. Huisgen, *Chem. Ber*. **1968**, *101*, 552.

REFERENCES

[1] R. Huisgen, in '1,3-Dipolar Cycloaddition Chemistry', Ed. A. Padwa, John Wiley & Sons, 1984, Vol. 1, p. 1 – 176; R. Huisgen, *Angew. Chem.*, *Int. Ed*. **1963**, *2*, 565; R. Huisgen, *Angew. Chem.*, *Int. Ed*. **1963**, *2*, 633.
[2] G. Steiner, R. Huisgen, *J. Am. Chem. Soc.* **1973**, *95*, 5056.
[3] R. N. Butler, A. G. Coyne, L. A. Burke, *J. Chem. Soc.*, *Perkin Trans. 2* **2001**, 1781.

[4] R. N. Butler, A. G. Coyne, W. J. Cunningham, L. A. Burke, *J. Chem. Soc.*, *Perkin Trans. 2* **2002**, 1807.
[5] R. N. Butler, W. J. Cunningham, A. G. Coyne, L. A. Burke, *J. Am. Chem. Soc.* **2004**, *126*, 11923.
[6] R. Huisgen, E. Langhals, *Tetrahedron Lett.* **1989**, *30*, 5369; R. Sustmann, W. Sicking, R. Huisgen, *J. Am. Chem. Soc*. **1995**, *117*, 9679; L. Fišera, R. Huisgen, I. Kalwinsch, E. Langhals, X. Li, G. Mloston, K. Polborn, J. Rapp, W. Sicking, R. Sustmann, *Pure Appl. Chem*. **1996**, *68*, 789.
[7] R. Breslow, D. Rideout, *J. Am. Chem. Soc*. **1980**, *102*, 7816.
[8] R. Breslow, *Acc. Chem. Res.* **1991**, *24*, 159.
[9] R. Breslow, C. J. Rizzo, *J. Am. Chem. Soc.* **1991**, *113*, 4340.
[10] M. R. Biscoe, R. Breslow, *J. Am. Chem. Soc.* **2003**, *125*, 12718.
[11] R. Breslow, *Acc. Chem. Res.* **2004**, *37*, 471.
[12] D. van Mersbergen, J. W. Wignen, J. B. F. N. Engberts, *J. Org. Chem*. **1998**, *63*, 8801.
[13] J. F. Blake, D. Lim, W. L. Jorgensen, *J. Org. Chem.* **1994**, *59*, 803; J. Chandrasekhar, S. Shariffskul, W. L. Jorgensen, *J. Phys. Chem. B* **2002**, *106*, 8078.
[14] T. R. Furlani, J. Gao, *J. Org. Chem*. **1996**, *61*, 5492.
[15] J. B. F. N. Engberts, *Pure Appl. Chem*. **1995**, *67*, 823; J. B. F. N. Engberts, M. J. Blandamer, *Chem. Commun.* **2001**, 1701.
[16] S. Otto, W. Blokzikl, J. B. F. N. Engberts, *J. Org. Chem*. **1994**, *59*, 5372.
[17] J. W. Wijnen, S. Zavarise, J. B. F. N. Engberts, *J. Org. Chem*. **1996**, *61*, 2001.
[18] R. Huisgen, *Angew. Chem.*, *Int. Ed*. **1980**, *80*, 947.
[19] R. N. Butler, M. O. Cloonan, *Bull. Soc. Chim. Belg.* **1997**, *106*, 515.
[20] R. N. Butler, *Irish Chem. News*, *J. Inst. Chem. Ireland* **1990**, *Autumn*, 12 – 14.
[21] S. Narayan, J. Muldoon, M. G. Finn, V. V. Fokin, H. C. Kolb, K. B. Sharpless, *Angew. Chem., Int. Ed.* **2005**, *44*, 3275.

Received February 24, 2005